Synthesis of $^{11}B_4C$ containing Ni/Ti multilayers and characterization using combined X-ray and neutron reflectometry

Sjoerd Broekhuijsen,[1] Fredrik Eriksson,[1] Naureen Ghafoor,[1] Martin Wess,[1] Alexei Vorobiev,[2] Jens Birch[1]

[1] *Department of Physics, IFM, Linköping University, SE-581 83 Linköping, Sweden*

[2] *Institut Max von Laue—Paul Langevin, 71 avenue des Martyrs, 38000 Grenoble, France*

Abstract

The ultimate performance of Ni/Ti neutron multilayer mirrors is crucially dependent on a high optical contrast and a minimal achievable layer thickness in the multilayers. However, these are currently limited by a finite interface width between the individual layers. As the reflectivity of a multilayer depends exponentially on the square of the interface width, even a modest improvement of these factors can lead to a significant increase in reflectivity performance of neutron optical components such as neutron supermirrors.

In this work we have incorporated low-neutron-absorbing ^{11}B and C during deposition to inhibit the formation of nanocrystals and limit interdiffusion in Ni/Ti multilayers. To overcome accumulated roughness caused by limited adatom mobility we employed a modulated ion-assistance scheme during magnetron sputter deposition in which the initial part of each layer is grown with a low substrate bias voltage of -30 V while the remainder of the layer is grown using a higher bias of -100 V. This modulates the energy of ions attracted from the process plasma in a way that minimizes intermixing into the previous layer and then stimulates adatom mobility to create a smooth top surface before deposition of the next layer [2].

Multilayers deposited with and without $^{11}B_4C$ co-sputtering have been investigated using a combination of Elastic Recoil Detection Analysis (ERDA) to determine the composition, and X-ray reflectivity (XRR) and neutron reflectivity (NR) for structural analysis and to determine reflectivity performance. A model representing the samples has been created using the GenX reflectivity fitting software [3], and the relevant structural parameters are fitted simultaneously to both X-ray and neutron reflectivity data. The resulting fit shows an elimination of accumulated roughness for the samples containing $^{11}B_4C$, as well as a higher overall neutron reflectivity, whereas the sample with pure Ni/Ti has a roughness accumulation of 0.03 Å per bilayer. The nominal interface width of the samples has been found to be 4.5 Å, compared to the current state-of-the-art of 7 Å [1]. TEM measurements on these samples are in agreement with the parameters found by the fitted XRR and NR data. Simulations based on these achieved interface widths suggest the total neutron transmission for a typical Ni/Ti supermirror waveguide with 10 reflections to increase with more than 7 times, therefore offering promise for significantly improved neutron flux at (future) neutron instrument stations.

Introduction

Neutron scattering is a non-destructive analytical technique which can be a powerful tool to investigate a range of physical properties. This technique offers some interesting advantages, among others for the study of bulk materials, magnetic properties and condensed matter. Neutron scattering however is a signal-limited technique providing relatively few neutrons to the experiment. The European Spallation Source, which is currently under construction, will have the world's most powerful neutron source, providing 100 times higher flux than the currently most brilliant source [ref]. Nevertheless, even the most brilliant neutron sources have a flux that is orders of magnitudes lower than the attainable flux for e.g. X-rays at synchrotron radiation sources. Instead, the largest

increase in neutron flux at the experiment is expected to come from improving the performance of neutron optical components [ref].

Most key components used in neutron scattering experiments utilize so called multilayer mirrors, and Ni/Ti is the most conventional choice for neutron multilayer mirrors because of the prospects of a high theoretical reflectance. The reflectivity performance of such mirrors critically depend on the quality of the interface structure. Assuming the variation in scattering length density (SLD) across the interface can be described by an error function, the reflectivity reduction caused by the interface width is accounted for by introducing a Debye-Waller factor,

$$R = R_0 e^{-\left(2\pi m \frac{\sigma}{\Lambda}\right)^2}$$

where s is the interface width and L the multilayer period. It follows even a modest improvement can lead to a significant increase in the reflectivity performance since the reflectivity is exponentially dependent on the square of the interface width. The interface width between the layers in a multilayer is caused by a combination of nanocrystallites, formation of intermetallics, intermixing, and interdiffusion between sequent layers in the mirror [1].

Here we need a literature review of what others have done – for Ni/Ti, to reduce interface widths, to characterize interface widths!

In this work we have investigated used a novel magnetron sputter growth technique with a special emphasis to reduce the interface width in Ni/Ti multilayers with the aim of increasing the neutron reflectance and thereby achieving a higher neutron flux at the experiment.

By incorporating low-neutron-absorbing $^{11}B_4C$ during deposition it was found that the formation of nanocrystals was inhibited and amorphous Ni/Ti multilayers were obtained. The addition of $^{11}B_4C$ limits the adatom surface mobility during the sputtering process and deposited atoms stick directly to the landing sites creating rough layers. To compensate this a modulated bias scheme was used during the deposition [ref to my article].

By summarizing what has been done, we come to what has not been done! I.e. our work! We have investigated Ni/Ti+$^{11}B_4C$ and determined the interface width (evolution) using a combination of X-ray and neutron reflectivity and compared that to ordinary Ni/Ti. Based on this we predict the supermirror performance.

Multilayers deposited with and without $^{11}B_4C$ co-sputtering have been investigated using a combination of Elastic Recoil Detection Analysis (ERDA) to determine the composition, and X-ray reflectivity (XRR) and neutron reflectivity (NR) for structural analysis and reflectivity performance. Initial findings show a significant increase of reflectivity at the first Bragg peak as well as a total elimination of accumulated roughness for the samples containing $^{11}B_4C$.

Experimental details

In this work, Ni/Ti multilayers have been deposited with and without $^{11}B_4C$ co-deposition. Both the samples with and without $^{11}B_4C$ have been compared to each other in terms of structural parameters and reflectivity performance. The samples were deposited at a ultra-high vacuum (UHV) magnetron sputtering chamber at PETRA III at the Deutsches Elektronen-Synchrotron in Hamburg, Germany [ref Schroeder, Birch 2015]. The cylindrical deposition chamber has a diameter of 600 mm and four 75-mm diameter sputter sources tilted with an angle of X° towards the substrate normal. A m-metal shielding is placed between the sputtering sources in order to extend the magnetic field closer to the substrate and minimise cross contamination. In front of the sputtering targets, fast-acting shutters are mounted to control the sputtering flux, enabling the growth of multilayers as well as the co-deposited samples grown in this work. The substrate table is electrically isolated in order to enable a negative substrate bias during film growth.

The samples have been deposited on 10×10×0.5 mm^3 Si (001) substrates with a native oxide that were rotated around the sample normal at a constant rate of 7 rpm during the growth process. The samples were deposited at ambient temperatures with no substrate heating. Ultra-high purity argon gas (> 99.999998%) has been used as sputtering gas at a working pressure of 3 mTorr (0.4 Pa), as measured by a capacitance manometer. The sputtering targets had a constant power of 20 W and 60 W for Ni and Ti, respectively, while 35 W was used for the $^{11}B_4C$ target. For the pure sample this resulted in a deposition rate of 0.376 and 0.427 nm/s for Ni and Ti, respectively, as determined by hard X-ray reflectivity measurements of single layer films. The samples that have been co-deposited with $^{11}B_4C$ showed a sputtering rate of 0.415 and 0.472 nm/s for the sample containing Ni and Ti, respectively.

The samples have been measured using various characterization techniques in order to investigate the structural properties. Apart from the inclusion of $^{11}B_4C$, both samples have been deposited in the same system under the same conditions as described above. Both samples have a total of 104 bilayers, with multilayer periods of 47.0 Å and 45.8 Å for the sample with and without $^{11}B_4C$, respectively.

The elemental composition of the films was determined using time-of-flight energy recoil detection analysis (ToF-E ERDA) at the Tandem Laboratory at Uppsala University. A primary beam of $^{27}I^{8+}$ was used with an energy of 36 MeV at an incident angle of 67.5° relative to the surface normal, the energy detector was placed at a recoil scattering angle of 45°. A detailed description of the experimental set-up is given elsewhere [ref]. The measured data has been analysed using the Potku software in order to determine the atomic concentrations [ref Potku].

An analytical Tecnai G2 UT FEG microscope operating at 200 kV for a point-to-point resolution of 0.19 nm was used for transmission electron microscopy (TEM) studies. Microstructure and layer definition of Ni/Ti and Ni/Ti doped with $^{11}B_4C$ multilayers were studied using both bright field and dark field imaging as well as high resolution cross-sectional TEM. Dark field imaging was used as an approach to effectively highlight crystalline regions in the sample, while high-resolution TEM was used to investigate the layered structure in the multilayers containing the thinnest periods. The cross-sectional samples were prepared using mechanical grinding and polishing followed by low-energy ion-beam milling using a Gatan precision ion polishing system.

Neutron reflectometry measurements were performed for a series of samples at Institut Laue–Langevin in Grenoble with the SuperAdam refractometer at a monochromatic wavelength of 5.23 Å. The distance from the sample to detector was 150 cm. Both the specular and off-specular signals were obtained simultaneously in this set-up. The pure Ni/Ti sample has been measured in a range of 0°-10° θ with a step size of 0.01°/step using a constant collection time of 50 s per step, leading to a total acquisition time of ~13.9 h. For the sample that has been co-deposited with 11B4C, the measurement has been split up in four different regimes. The first regime was performed in a range of 0-1° θ with a step size of 0.005°/step and an acquisition time of 30 s per step. The second regime was done from 1–4° θ with a step size of 0.01°/step and a collection time of 40 s per step. The third regime was performed from 4–7° θ with a step size of 0.02°/step and a collection time of 80 s per step. The fourth and final regime was performed from 7-15° θ with a step size of 0.04/step and a collection time of 150 s per step. The total acquisition time for this sample was ~16.7 h. Footprint correction has been applied to both samples for the specular signal using the provided data reduction software at instrument site. For this correction, a trapezoid beam was assumed after which the total data set has been normalised to the critical angle.

X-ray reflectivity measurements were performed using a Panalytical Empyrean diffractometer using a Cu X-ray tube. On the primary side, a parallel beam X-ray mirror has been used in combination with a 1/32° divergence slit, while a parallel plate collimator has been used in combination with a collimator slit on the refracted side with a PIXcel-3D area detector in 0D mode. Reflectivity of the multilayers were measured in the range 0°-10° 2θ with a step size of 0.01°/step and a collection time of 0.88 s per step, giving a total measurement time of ~30 minutes.

Structural analysis was performed by fitting the obtained X-ray and neutron reflectivity data simultaneously to a model created with the GenX reflectivity fitting software which uses the Paratt recursion formalism to simulate specular reflectivity [ref GenX]. All samples are described using the same model description. A stack of a fixed amount of bilayers on top of a Si substrate. Based on observations from TEM-measurements, a thin layer of native SiO_2 is included on top of the substrate, as well as a thin layer of NiO on top of the multilayer stack.

Results and discussion

Transmission electron microscopy of both samples show smooth interfaces throughout the multilayer. While some roughness correlation can be observed, any obvious roughness accumulation is not present in either of the samples. Bright field TEM micrographs are shown in figure X. Some crystallinity can be observed for the $^{11}B_4C$ doped sample…

Compositional analysis has been performed using ERDA in order to obtain the $^{11}B_4C$-content in the samples that were co-deposited with $^{11}B_4C$. These samples show 21.9% Boron and 3.59% Carbon in the sample. Using the deposit times for each layer, it can be calculated that the Ni-layer contains 19.7 and 3.2 % ^{11}B and C respectively, while the Ti-layer contains 24.5% and 4.0% ^{11}B and C respectively.

Neutron reflectivity measurements were performed to investigate structural parameters of the samples. The specular signal for the pure Ni/Ti sample is compared to the sample that was co-deposited with $^{11}B_4C$ in figure Y. A clear increase in specular reflectivity can be observed at the first Bragg peak, the lower reflectivity can be explained by a difference in the thickness-ratio for each bilayer. Unlike the higher order peaks, which are strongly dependent on this ratio, the reflectivity at the first Bragg peak is mostly unaffected by this ratio making it a better indicator for a low interface width.

The off-specular signal is collected simultaneously with the specular signal, these measurements are shown in figure Z. Both samples show a clear Bragg sheet around the first Bragg peak, which indicates some correlation between the layers. A weak but non-negligible Bragg-sheet can also be observed around the second Bragg peak of the pure Ni/Ti sample. This could possibly attributed to a stronger correlation between the layers. Rocking curves around the first Bragg peak have been obtained by integrating over the measured Q_x range at the first Bragg peak. It should be noted that the observed diffuse signal, shown in the inset of figure Yb, is larger for the $^{11}B_4C$ containing sample. This can possible be attributed to a low intermixing between the subsequent layers for these samples. This leads to a locally stronger contrast in SLD, even for a lower overall interface width. The diffuse signal would therefore be magnified, even if the layers are not necessarily more correlated.

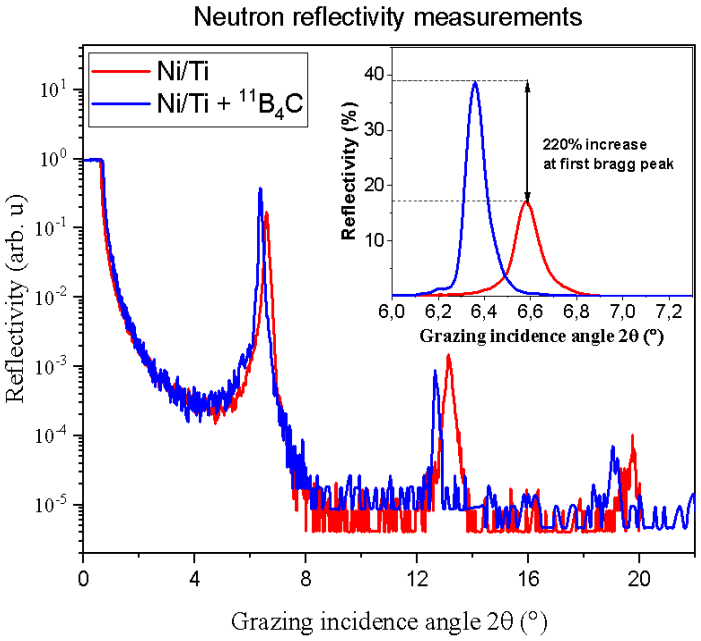

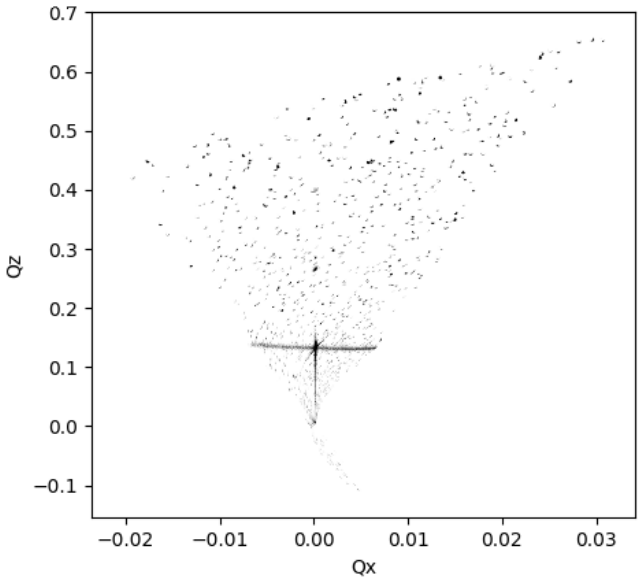

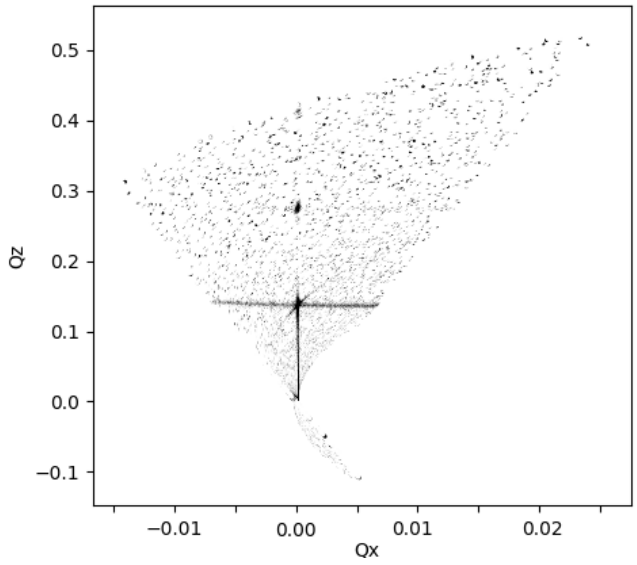

To obtain structural parameters, a combination of experimental X-ray and neutron measurements have been fitted to a simulated model. This has been done both for the pure Ni/Ti samples and for the 11B4C containing Ni/Ti samples. The model assumes an independent initial interface width for both layers in each bilayer, while a linear accumulation in interface width is introduced as a fitting parameter. The interface width accumulation is considered equal for both layers. The interface width for the Ni- and Ti containing layer in the i'th bilayer in the multilayer is therefore determined by

$$\sigma_{Ni,i} = A \cdot i + \sigma_{Ni,initial} \text{ and } \sigma_{Ti,i} = A \cdot i + \sigma_{Ti,initial},$$

where A is the increase in interface width per bilayer, i.e. describing a roughness accumulation, the letter i indicate bilayer position in the stack from the substrate, and $\sigma_{Ni,initial}$ and $\sigma_{Ti,initial}$ describe the initial interface width for the Ni- and Ti containing layer respectively.. A sketch of this model can be seen in figure 1.

Figure 1. An illustration of the sample as described in the simulated model, not to scale. Each bilayer is given an index, dubbed i. For illustrative purposes only a limited amount of bilayers are drawn.

The samples also show a small increase of interface width throughout the layer, which leads to a slight peak broadening at higher angles. This has been incorporated into the model by allowing the layer thickness for each layer to increase linearly for each bilayer, similar to the interface width. In order to restrict the number of fitting parameters, the interface drift is modelled as being equal for both bilayers. The thickness of each layer is therefore described as

$$\mathrm{d_{Ni}} = \mathrm{D} \cdot j + \Gamma \cdot \Lambda \text{ and } d_{\mathrm{Ti}} = \mathrm{D} \cdot \mathrm{i} + (1 - \Gamma) \cdot \Lambda,$$

where D describes the increase in thickness per bilayer, i indicates the position of the bilayer in the stack, Γ is a dimensionless number indicating the ratio between the thicknesses in the bilayer and Λ is the total thickness of the first bilayer. The scattering length density (SLD) for each layer depends both on the elemental composition, and on the density of the layer. The SLD of each bilayer in the sample has therefore been calculated by summing over each element in the layer using the following expression

$$\mathrm{SLD} = \frac{\rho N_a \sum_{j=1}^{N} c_j b_j}{\sum_{j=1}^{N} c_j M_j},$$

where ρ denotes the mass density of the layer and $\mathrm{N_a}$ is Avogadro's number. The elemental concentration in the layer, the scattering length and the molecular weight for each element are described by $\mathrm{c_j}$, $\mathrm{b_j}$ and $\mathrm{M_j}$ respectively. The density for each bilayer has been calculated using a linear interpolation from the bulk densities for each element, while the compositional values are retrieved from ERDA measurements. The resulting SLD for the individual layers in each sample are given in table 1. The structural properties of the samples are fitted for within a reasonable range from the expected values given the XRR and NR data. The resulting parameters are summarised in table 1 and table 2.

Table 1: The SLD that has been calculated for the different layers in the sample for reflectivity simulations in this work. The imaginary component of the SLD for neutrons was negligible for all layers. (I do not know how to make table captions in MS word)

Layer	**Neutron SLD ($Å^{-2}$)**	**X-ray SLD ($Å^{-2}$)**
NiO	8.658	50.125 - 3.002i
Ni	9.414	65.465 - 1.350i
Ti	-1.949	35.518 - 0.847i
Ni + $^{11}B_4C$	8.848	53.969 - 1.067i
Ti + $^{11}B_4C$	-0.350	30.935 - 2.392i
SiO_2	4.186	22.724 - 0.294i
Si	2.0648	19.984 - 0.456i

Table 2. Obtained structural information for both multilayers.

Parameter	**Pure Ni/Ti**	**Ni/Ti+$^{11}B_4C$**
Multilayer period Λ	45.8 Å	47.0 Å
Layer thickness ratio, Γ	0.48	0.50
Initial interface width for the Ni-layer, $\sigma_{Ni,initial}$	8.9 Å	5.6 Å
Initial interface width for the Ti-layer, $\sigma_{Ti,initial}$	2.8 Å	3.4 Å
Accumulated roughness	0.04 Å/bilayer	0.00 Å/bilayer

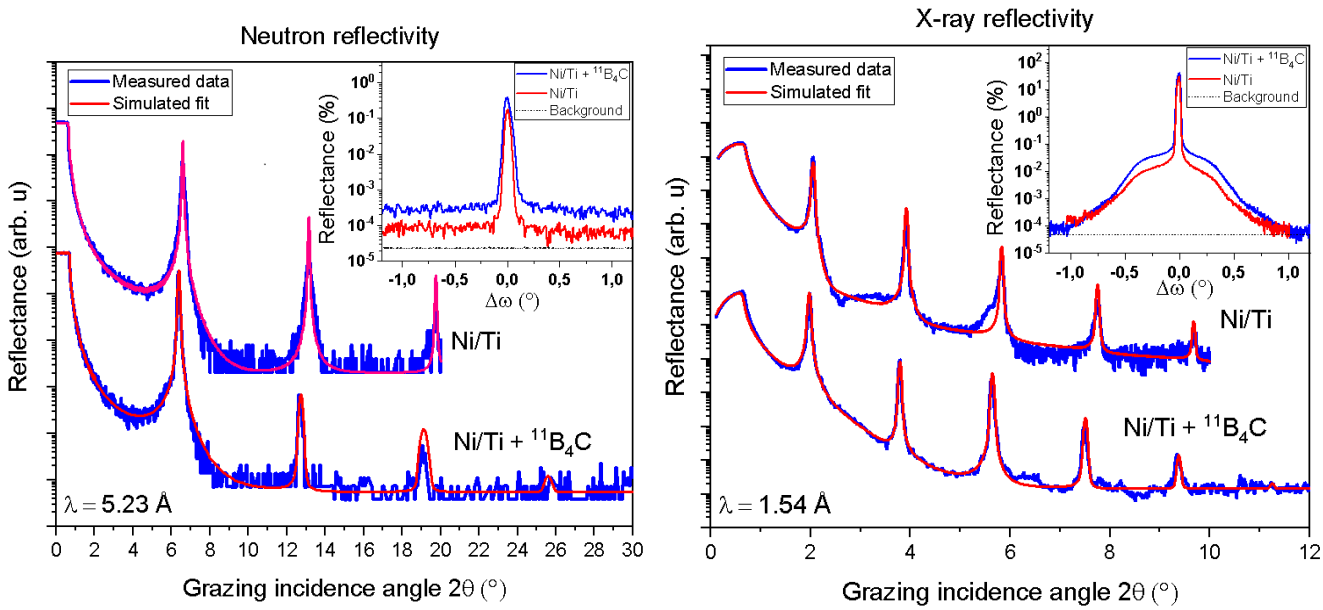

Figure X shows the experimental X-ray and neutron reflectivity measurements, as well as a simulated fit to the specular data. The off-specular signal can be seen in the insets in the right-hand corner. Despite showing less roughness accumulation per bilayer in the fitted model, the samples with $^{11}B_4C$ do show a stronger diffuse signal than the pure samples, this is observed in both the neutron- and X-ray reflectivity measurements. The pure Ni/Ti sample also shows clear signs of oxidation both in the TEM measurements, as well as in the fitted simulations, whereas the sample that has been co-deposited with $^{11}B_4C$ didn't show any signs of oxidation at all. The theoretical model has been fitted to the XRR and NR data simultaneously using and is in excellent agreement with the experimental data. The structural parameters that follow from these fits are shown in table 2. The mean initial interface width, which is defined as the mean value of the interface width in the first bilayer in the sample, was shown to be 6.3 Å for the pure Ni/Ti multilayer. The mean initial interface width for the $^{11}B_4C$ containing Ni/Ti multilayer was found to be 4.5 Å. The pure Ni/To sample also showed a roughness accumulation equal to 0.04 Å per bilayer, whereas the $^{11}B_4C$ containing Ni/Ti sample didn't show any signs of roughness accumulation at all. An overall increase in layer thickness of about 0.002 Å per bilayer could be observed in both samples, which is most likely attributed to the deposition system itself.

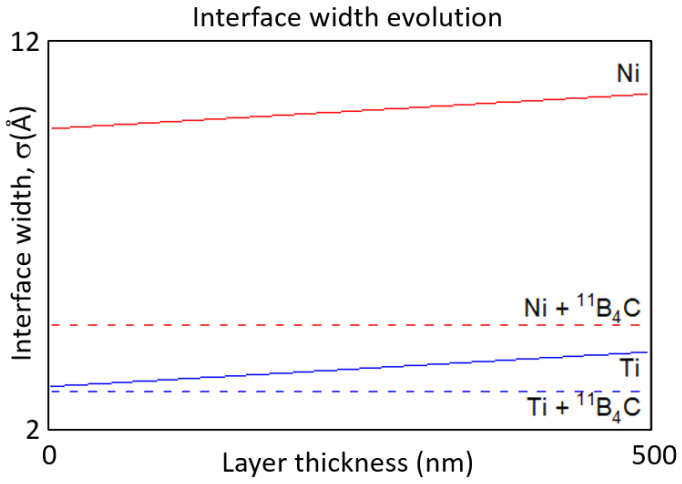

The current state of the art for Ni/Ti multilayers used in neutron supermirrors have an interface width of about 7 Å, the obtained widths in this work therefore offer a clear improvement. The theoretical performance of such multilayers in neutron supermirrors have been calculated using the IMD software. The same structural properties were used as found in the deposited samples discussed in this work, where the SLD has been calculated using the elemental composition as obtained by ERDA. The multilayers are simulated with an increasing bilayer period from 20 Å to 400 Å, a neutron wavelength of 3.0 Å and a total of 5000 bilayers. The simulated reflectivity performance is shown in figure X. For a typical m = 6 neutron mirror, an increase in reflectance can be observed from 0.64 to 0.72, resulting in a reflectance of 0.012 and 0.037 after 10 reflections for these respective samples, which is an increase of more than 300%.

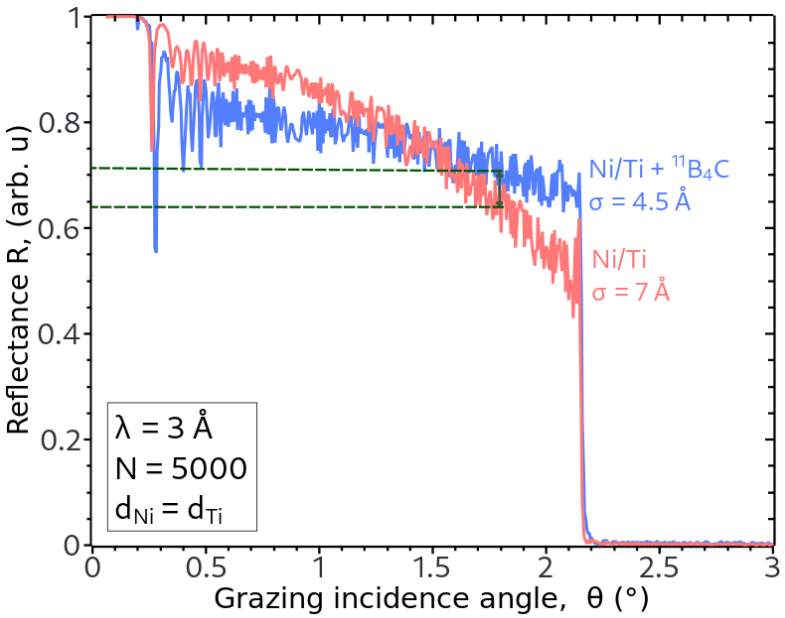

Conclusions

In this work we investigated a novel magnetron sputter growth technique where $^{11}B_4C$ co-deposition has been combined with a split-bias scheme in order to reduce interface width at Ni/Ti multilayers. Combined fits to experimental XRR and NR data indicate average interface widths in each bilayer of 4.5 Å without any accumulated roughness when the sample is co-deposited with $^{11}B_4C$. This is a significant reduction from the deposited sampled with pure Ni/Ti, which show an average initial interface width in each bilayer of 6.3 Å with an accumulation of 0.04 Å per bilayer. The obtained interface width offers very good prospects for high-performance supermirrors with high-m values, as well as for neutron instruments for cold neutrons where thinner interface widths are required. Since neutron multilayers are such essential and crucial elements in any intended instrumentation, even the slightest improvement of the performance will have an immediate and large impact on all research using those instruments.

Acknowledgements

Definitely SFF for funding, UU for ERDA measurements. Should SwedNess as a whole be mentioned here?

References

[11] D.L. Windt, IMD—Software for modelling the optical properties of multilayer films, Computers in Physics, 12 (1998).

An ideal sample with abrupt and flat interfaces will be constant in terms of scattering potential in the in-plane direction for the entire layer. For a non-ideal sample with surface roughness, local differences in chemical composition occur in the in-plane direction of the sample. The parallel component of the neutron beam is therefore subject to a potential barrier, leading to partial refraction into the in-plane direction. This off-specular scattering provides information about the roughness profile at the interfaces. Interface roughness for instance gives rise to sharp local scattering potential barriers in the off-specular direction, and therefore contributes to the off-specular signal. Intermixing however leads to a more gradual contrasts in the in-plane direction and contributes therefore much less to the off-specular signal. A strong off-specular signal is therefore often the result of surface roughness instead of intermixing, a distinction that cannot be made with purely specular scattering.